6.4

COUPLING BETWEEN LAND-SURFACE, BOUNDARY-LAYER PARAMETERIZATIONS AND RAINFALL ON LOCAL AND REGIONAL SCALES: LESSONS FROM THE WET SUMMER OF 1993.

Alan K. Betts and John H. Ball
Atmospheric Research
Pittsford, VT 05763

A.C.M. Beljaars, M.J. Miller, and P. Viterbo
ECMWF, Reading, England

1. INTRODUCTION

In this paper we discuss the impact of the coupling between the land-surface, boundary-layer (BL) parameterizations and rainfall on two different time and space scales: a local diurnal timescale and a regional seasonal timescale. The catastrophic flooding in the continental mid-West of the US in the summer of 1993 focused our attention on the coupling between soil moisture and rainfall on long-time scales, just as Cycle 48 of the ECMWF model was implemented. The development of cycle 48 of the ECMWF model was based extensively on the use of local test data-sets, including FIFE-1987 (Betts et al, 1993, Beljaars and Betts, 1992; Beljaars 1993). It included four predictive layers for soil moisture, as well as other changes discussed briefly below. We discovered a large sensitivity of *monthly and seasonal* precipitation over the US on initial soil moisture. Because of the profound importance of this on long-term rainfall prediction, we are presenting some preliminary results and a brief discussion of some of the feedbacks involved. This research has been further stimulated by the planning needs of the GCIP and BOREAS field programs, which address respectively the interaction between the surface and atmosphere for the Mississippi basin, and a cross section of the Canadian boreal forest between Saskatchewan and Manitoba.

We shall first illustrate the local diurnal feedback using the FIFE data, and a simple mixed boundary layer (BL) model. These show the dependence of the surface diurnal cycle of θ, q and θ_E on soil moisture and BL entrainment. Greater soil moisture leads to a higher afternoon maximum of θ_E, as does reduced entrainment. The diurnal cycle of θ_E is in turn linked to precipitation and cloudiness. We then show an idealised mixed layer model comparison, which illustrates how drier soil moisture and increased BL entrainment have similar impacts on the BL diurnal evolution, of θ and q. The partition of the net surface radiation into sensible and latent heat fluxes does not affect the surface θ_E flux, but it does impact both entrainment of low θ_E air and BL-depth.

We then discuss the larger regional scale feedback using two T-106 30 day forecasts using cycle 48 of the ECMWF model, initialized with the same atmospheric data of July 1 1993, but with different initial soil moistures: one dry, one wet. These show that a large increase in the monthly mean precipitation over the central US results from an increase of initial soil moisture. The forecast precipitation from the initially wet soil moisture is remarkably similar to the anomalous high precipitation observed. This suggests that monthly mean rainfall over land is correlated on large scales with initial soil moisture, and may therefore have some predictability.

* *Corresponding author address:* Alan K. Betts, Atmospheric Research, RR#3, Box 3125, Pittsford, VT 05763.

2. LOCAL INTERACTIONS

2.1 Background

Several field programs over land: BOREAS (Boreal Forest Ecosystem and Atmosphere Study), GCIP (GEWEX Continental scale International Project) and ARM (Atmospheric Radiation Measurement) plan measurements to validate and improve parameterizations in large-scale models. This section addresses the local coupling between the land-surface and boundary layer parameterizations. One objective is to show the key role of soil moisture. The second is to clarify why daytime measurements of the diurnal cycle of the atmosphere boundary layer (ABL) are needed by these experiments: it is because of uncertainties in entrainment (Betts et al, 1992, Betts and Ball, 1993).

Sellers and Hall (1992: Fig 10) in their FIFE review, present one mainstream view of the problem. They discuss how soil moisture might be tuned in GCM's to reproduce an observed surface time-series of temperature and humidity. In the process they presume this will give the correct surface fluxes. This argument is incomplete. Soil moisture does play a major role in determining the surface evaporation, but so does the growth of the daytime ABL which mixes down warm, dry air at BL-top. A GCM may closely reproduce the 2-m time-series of temperature and humidity (say θ and q), but have both the wrong surface fluxes and soil moisture, if its parameterization of the BL-top entrainment process is significantly in error. The time-series of (θ,q) at 2m (and in the mixed layer) results from an imbalance between surface fluxes and BL-top entrainment fluxes. Increasing these entrainment fluxes (the coupling with the free atmosphere); which increases the warming and drying of the ABL, is difficult to distinguish from the effect of low soil moisture, which shifts the partition of the surface available energy from latent to sensible heating. The surface fluxes and entrainment, however, have different impacts on the θ_E balance of the BL. The surface θ_E flux is related to the net radiation (RNet) at the surface (which is primarily affected by season and cloudiness), so that for a given RNet, changes in soil moisture do not affect the surface θ_E flux. Entrainment introduces low θ_E air into the BL. Increasing entrainment by any means (including increasing the surface sensible heat flux which drives more entrainment), reduces BL θ_E. The θ_E equilibrium of the BL is a critical control on convection on local and regional scales. Shallow convection also transports high θ_E air out of the sub-cloud layer, and precipitation from deep convection finally moistens and cools the surface and restabilizes the BL through downdrafts. In this section we shall explore some of these interactions using FIFE data and a simple model.

2.2 FIFE Averages

We illustrate the local diurnal variation using four averages from July and early August, 1987 FIFE surface data, near Manhattan, Kansas. Table 1 shows the data used, the mean maximum surface Bowen ratio and the maximum total surface heat flux (RNet-ground heat flux) (derived from the data of Smith et al, 1992). The surface Bowen ratio is a maximum just after local noon.

Table 1

FIFE Diurnal averages by surface Bowen ratio.

Days in average	Max surface Bowen ratio	Max surface (RNet-Grnd) (Wm^{-2})
July 6, 9-11	0.35	562
July 18-20	0.54	562
July 23-27	0.78	525
July 28-Aug 2	0.89	513

It rained on July 5, 7, and 8; so the days in the first average are when the soil is wet, and the surface Bowen ratio is correspondingly low. It rained again July 17-18 (before sunrise on the 18th), and then in the period running till Aug 2, there was no rain. The soil dried steadily and the surface Bowen ratio rose steadily (Kim and Verma, 1990). Fig 1 shows the day-time diurnal cycle on a (θ,q) plot from 1145 Z (just after sunrise) to 2345 Z. The data are half-hour averages. These 4 averages illustrate the changing diurnal cycle with decreasing soil moisture and rising surface Bowen ratio, in a progression from right to left. For the low surface Bowen ratio average on the right, θ and q rise during the day, and reach a maximum in the afternoon (near 1300 L or 1915 Z), before the surface starts to cool. θ_E reaches a maximum of about 364K (see dashed isopleths) at this time. Moving left across Fig 1, each subsequent average (with higher surface Bowen Ratio) reaches a warmer drier afternoon maximum, but at a lower θ_E. With the driest soil, for which the surface Bowen ratio maximum is 0.89, the maximum temperature is the highest, but the BL is driest, and the θ_E maximum is the lowest, only ≈ 353K (reached at the surface before local noon). The primary reason for this trend of maximum θ_E is not the surface θ_E flux. The maximum net radiation minus ground heat flux does decrease from 562 to 513 Wm^{-2} with increasing surface Bowen ratio (Table 1), because the net longwave (out) increases with the warmer surface and drier atmosphere above: so there is therefore a small decrease in the surface θ_E flux. However there is a large increase in the entrainment of dry (low θ_E) air into the BL, driven by the increase in surface heat flux with increasing surface Bowen ratio. The simple mixed layer model in the next section will confirm this analysis quantitatively.

Note that the initial condition near sunrise for each average is also shifted, presumably because on successive days of high (or low) evaporation, the BL moistens (or dries); but there is little difference in the morning temperature minimum, which is controlled by the radiative balances over the whole day (not discussed here).

2.3 Mixed layer model

An idealized set of calculations based on the mixed layer equations from Betts (1992) will quantify these local interactions. We ignore horizontal advection as a climatological simplification. The inversion base virtual heat flux is related to the surface virtual heat flux using an entrainment coefficient A_R as a closure [Betts, 1973; Carson, 1973; Tennekes, 1973]

$$F_{i\theta_v} = -A_R\, F_{s\theta_v} \tag{1}$$

Here F denotes a heat flux in watts per square meter. The local changes of mixed layer θ_m and q_m are given in terms of the flux difference between the surface (subscript s) and the inversion (subscript i)

$$C_p\ \partial\theta_m/\partial t = g(F_{s\theta}-F_{i\theta})/\Delta p_i \tag{2a}$$

$$L\ \partial q_m/\partial t = g(F_{sq}-F_{iq})/\Delta p_i \tag{2b}$$

where Δp_i (defined positive) is the pressure depth of the mixed layer. Defining surface and inversion level Bowen ratios (β_s and β_i), and using the closure (1) gives (see Betts (1992)

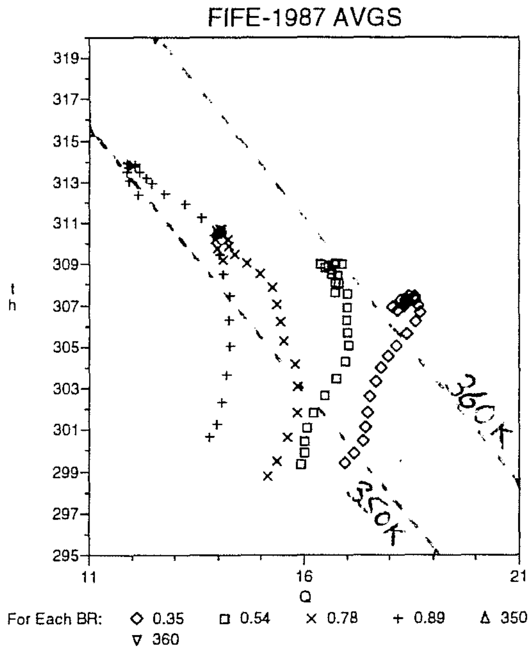

Figure 1: Daytime (θ,q) path for FIFE 2-m averages from 1145Z to 2345Z for 4 surface Bowen ratios. θ_E lines are dashed.

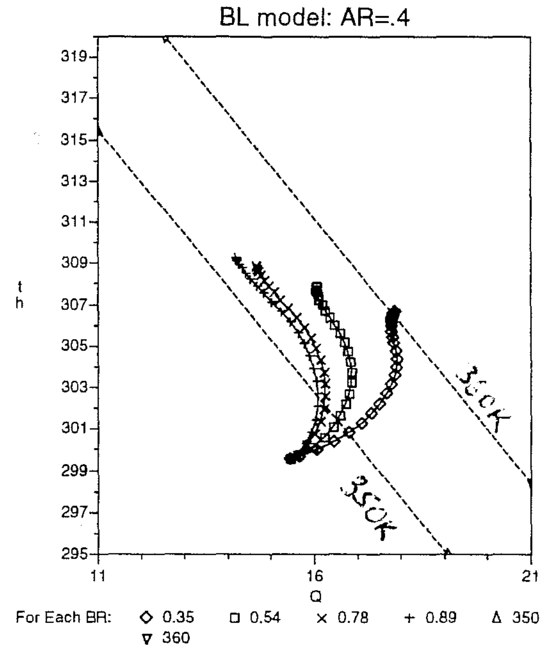

Figure 2: Mixed layer model solution as function of surface Bowen ratio. Entrainment parameter A_R=0.4.

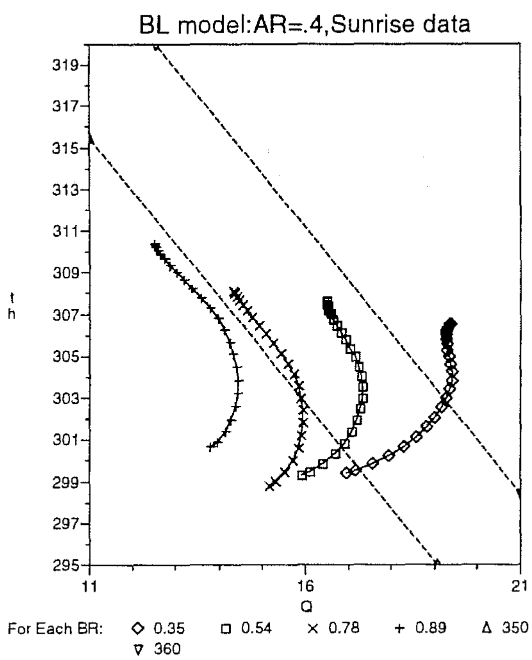

Figure 3: As fig 2, starting with Fig 1 initial states of (θ,q) just after sunrise.

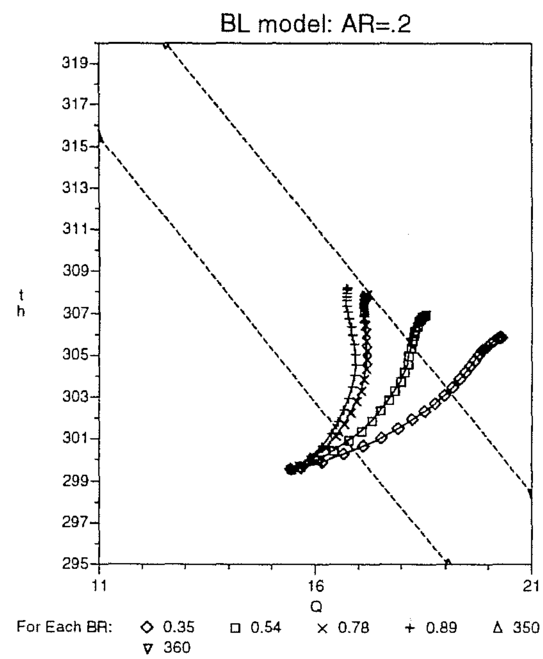

Figure 4: As Fig 2 with lower entrainment parameter A_R =0.2

$$C_p \frac{\partial \theta_m}{\partial t} = g \frac{F_{s\theta}}{\Delta p_i}\left[1 + \frac{\beta_i}{\beta_s} A_R \frac{(\beta_s - \beta_v)}{(\beta_i - \beta_v)}\right] \quad (3a)$$

$$L \frac{\partial q_m}{\partial t} = g \frac{F_{sq}}{\Delta p_i}\left[1 + A_R \frac{(\beta_s - \beta_v)}{(\beta_i - \beta_v)}\right] \quad (3b)$$

where $\beta_v \approx -0.07$ is the slope of the dry virtual adiabat.

The leading terms in (3a) and (3b) are just the surface fluxes, which warm and moisten the ABL. The second pair of terms, proportional to A_R, are the entrainment fluxes of typically warm, dry air at the inversion. If we introduce the surface energy balance

$$\text{RNet-Grnd} = F_{s\theta} + F_{sq} \quad (4)$$

we can solve (3) and (4), given Δp_i. A simple solution for the growth of BL depth, Δp_i, can be found by assuming the inversion strength $(\Delta\theta)$ at BL top to remain constant

$$\Delta\theta = \theta^+ - \theta_m = constant \quad (5)$$

where θ^+ (just above inversion) increases as the BL deepens. Then

$$\frac{\partial \theta_m}{\partial t} = \frac{\partial \theta^+}{\partial t} = \Gamma^+ \frac{\partial \Delta p_i}{\partial t} \quad (6)$$

where $\Gamma^+ = -(\partial\theta/\partial p)^+$, just above the BL top inversion (we neglect the small (and partly canceling) effects of subsidence and radiative cooling on changing θ^+ and Δp_i). Combining (3a), and (3b) gives $\partial\theta_{Em}/\partial t$ for the mixed layer as

$$C_p \frac{\partial \theta_{Em}}{\partial t} = g \frac{F_{s\theta_E}}{\Delta p_i}\left[1 + A_R\left(\frac{\beta_s - \beta_v}{\beta_i - \beta_v}\right)\left(\frac{\beta_i - \beta_w}{\beta_s - \beta_w}\right)\right] \quad (7)$$

where $F_{s\theta_E} \approx F_{s\theta} + F_{sq}$, if we approximate $\theta/\theta_E \sim 1$. This second constant in (7), $\beta_w \approx -1$ comes from the slope of the wet adiabat (Betts, 1992).

Eqs. (3a), (3b) and (6) can be integrated from an initial morning condition (we used $\Delta p_i = 10$ mb), to give the profile of (θ_m, q_m) during the day. Note that the slope $\partial\theta_m/\partial q_m$ is only a function of A_R, β_s and β_i. If these are constant, so is $\partial\theta_m/\partial q_m$.

Fig 2 shows the numerical integration from a fixed initial condition at sunrise for the four surface Bowen ratios, β_s in Table 1, with all other parameters identical. A 30-min time-step was used. Table 2 shows the simple analytic functions for the surface heating and the diurnal dependence of β_s, β_i, which we used to approximate the FIFE July and August BL data in Betts and Ball, 1993. A 12-hr daylight period was used, and time after sunrise is denoted by t.

Table 2
Idealized Model Parameters

RNet-Grnd:	$540(1-(t-6)^2)\,Wm^{-2}$
β_s:	$\beta_s(noon)\left(1-\frac{(t-6)^2}{49}\right)$
β_i $t<6.5$:	$-0.6(1-(t/12)^{0.7})$
β_i $t \geq 6.5$:	$-0.6(1-(6.5/12)^{0.7})$
Γ	$5\,K/100mb$

Fig 2 shows a similar dependence on Bowen ratio as Fig 1. With a higher surface Bowen ratio, the afternoon state is warmer and drier with a lower θ_E. Fig 3, (where we have integrated from the same morning conditions of θ,q as the Fig 1 data), matches Fig 1 better. The effect of the observed surface variation of net surface flux (Table 1) is very small (<0.5 K in θ_E), and we ignore it here. Fig 3 shows the mixed layer path of θ_m and q_m; while Fig 1 shows that of θ,q at about 2m in the superadiabatic layer: nonetheless they are very similar. Together Figs 2, and 3 suggest that about half the afternoon θ_E difference in Fig 1 is due to the difference of surface Bowen ratio alone, and the rest to the different mixing ratio at sunrise.

Earlier ECMWF comparisons with the FIFE data (Betts et al, 1993, Fig 12) had shown a similar impact of soil moisture on the local daytime cycle of (θ,q). The development of cycle 48 discussed in the next section shows that there is a major regional feedback of soil moisture on precipitation on larger timescales.

2.4 Effect of Entrainment parameter

Fig 4 is the same as Fig 2, but the entrainment parameter A_R has been reduced from 0.4 (the value found in FIFE) to 0.2 (the value used in many BL models). The reduced entrainment has a large impact on the afternoon (θ,q,θ_E) state. Indeed it is clear that the effects of higher β_s may be difficult to distinguish from lower A_R. For example the final state is similar for $\beta_s \sim 0.5$, $A_R \approx 0.2$ or $\beta_s \sim 0.35$, $A_R \approx 0.4$. Our FIFE analysis (Betts et al 1992, Betts and Ball, 1993) concluded that $A_R \approx 0.4$, but more coupled field studies of surface fluxes and BL entrainment are needed.

3. ECMWF FORECASTS FOR JULY 1993: REGIONAL INTERACTION.

The ECMWF model cycle 48 (Beljaars, 1993) introduced major changes to the land surface parameterization, as well as a new boundary layer parameterization and changes to the air-sea interaction formulation, following Miller et al, 1992. The changes over land were prompted by comparisons with field data (Betts et al, 1993; Beljaars and Betts, 1992). The changes most relevant to this paper were the introduction of four prognostic layers for the land surface hydrology, a new skin temperature and greater entrainment at the top of the unstable daytime BL.

The final "E-suite" testing of the ECMWF model cycle 48 started on July 1, 1993 and was followed by operational implementation in August. In retrospect, this was fortuitous in view of the subsequent catastrophic flooding in the Mississippi basin in July; because comparison of the old and new cycles of the model showed the impact of the new land surface parameterization in cycle 48. Furthermore, global initialization of the soil moisture was a key issue in starting the new model cycle; as it showed the sensitivity of forecasts to initial soil moisture. An attempt was made first to derive a global climate for soil moisture to initialize the new operational model by running the new model for four years at T-63 resolution, and averaging the four annual cycles. However, it was clear that this model "soil climate" was too dry, and the precipitation over land was too low in this 4-year run. It is believed that this results at least in part from long term interactions with errors in the incoming net radiation at the surface (probably coming in turn from too little cloudiness over land). Since this spring and summer were abnormally wet over parts of the central US of Europe, initializing the forecast model with too dry soil moisture fields produced large positive errors in the daytime temperature maxima over the summer continents. So a series of experiments were run with higher soil moisture fields using 1992 data, which showed a remarkable seasonal impact of soil moisture on precipitation. Specifying initially moist soils on May 1, 1992 gave almost double the summer (3-mo) precipitation over the central US (in 120 day T-63 runs), in comparison with forecasts initialized with the dry "climate" soil moisture. Consequently the soil moisture in vegetated areas was increased to field capacity to start the new operational model cycle 48 in August, 1993.

This prompted us to explore the impact of soil moisture on the July 1993 rainfall over the central US. Since cycle 48 analyses were available from July 1, 1993, we ran two one month forecasts from this date at T-106 resolution starting with the same atmospheric data, but different soil moisture. The "wet" forecast started with vegetated soils at field capacity. In the model, this gives "unstressed" evaporation by the vegetation. The second "dry" forecast had soil moisture set so that the vegetative resistance to evaporation was 4x the unstressed value. The impact on the July mean precipitation was remarkable in the central US. Fig 5 is the forecast (T2A) from the wet soil condition; Fig 6 (T3L) is from the dry soil condition. The monthly mean precipitation for the central US (in mm/day) from the initially wet soil simulation is roughly double that from the initially dry soil. Fig 7 shows the difference field between the two simulations: showing a mean increase of precipitation of 4mm day^{-1} over the central US, and decrease to the South over Texas. Fig 8 shows the actual July rainfall in inches from the NOAA Climate Analysis Center. The similarity of this precipitation pattern over the central US and Texas to the July simulation from wet soils (Fig 5) is striking (4 mm/day $\approx$ 5 inches/mo)), although the high precipitation in the monthly "forecast" (from a global model at T-106 resolution) does not extend as far south into Kansas and Missouri as was observed. The precipitation decrease over Alabama and Georgia, shown in Fig 7, mirrors the abnormally low rainfall in July in that region shown in Fig 8, although the "forecast" precipitation still exceeds that observed.

The increase in precipitation has not come from simply evaporating the **initial** soil moisture, since the differences in soil moisture are maintained for the month (not shown). The mechanism probably involves the higher BL θ_E over moist soils (shown in the previous section), the increase in convection and precipitation (tied to this higher moist adiabat) heating the atmosphere over a large enough horizontal scale to induce increased moisture convergence. This large-scale feedback is being studied further.

3. CONCLUSIONS

The result shown in Fig 7 is very significant, as it suggests that the coupling of BL equilibrium and precipitation with soil moisture has a long timescale, which may yield some long-term predictability in precipitation over the summer continents, provided we have adequate analyses of soil moisture. These were not available for the start of the ECMWF model cycle 48, (so the model was initialized with soil moisture fields that were partly assumed); but it is hoped that over the next fall, winter and spring the precipitation generated by the model initialization will generate and maintain realistic soil moisture fields.

Acknowledgements

AKB is supported by NSF under Grant ATM90-01960 and NASA-GSFC under contracts NAS5-31738, and NAS5-32334.

References

Beljaars, A.C.M, 1993: Model Cycle 48. ECMWF Research Dept. Memorandum. 44pp.

Beljaars, A.C.M. and A.K. Betts, 1992: Validation of the boundary layer representation in the ECMWF model. ECMWF Semina proceedings, Sept. 1992.

Betts, A.K., Non-precipitation cumulus convection and its parameterization, Q.J.R. Meteorol. Soc., 99, 178-196, 1973.

Betts, A.K., 1992: FIFE Atmospheric Boundary Layer Budget Methods. J.G.R., 97, 18523-18532.

Betts, A.K., R.L. Desjardins, and J.I. MacPherson, 1992: Budget analysis of the Boundary Layer grid flights during FIFE-1987. J.G.R., 97, 18533-18546.

Betts, A. K. and J.H. Ball, 1993: Budget analysis of FIFE-1987 sonde data. J. G. R. (conditionally

Thursday 1 July 1993 12z ECMWF Forecast t+744 VT: Sunday 1 August 1993 12z
SURFACE: Total Precipitation
fcap T2A

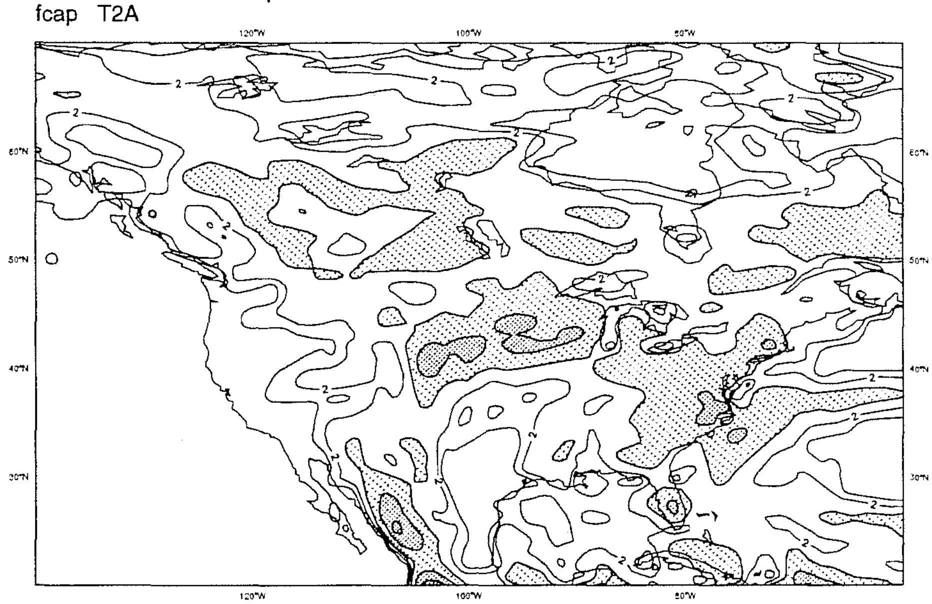

Fig 5 30-day average precipitation (mm/day) from ECMWF Cycle 48 T-106 forecast from July 1, 1993, using wet July 1 soil moisture, corresponding to unstressed evaporation. Contours are at 1, 2, 4, 8 mm/day.

Thursday 1 July 1993 12z ECMWF Forecast t+744 VT: Sunday 1 August 1993 12z
SURFACE: Total Precipitation
0.25ava T3L

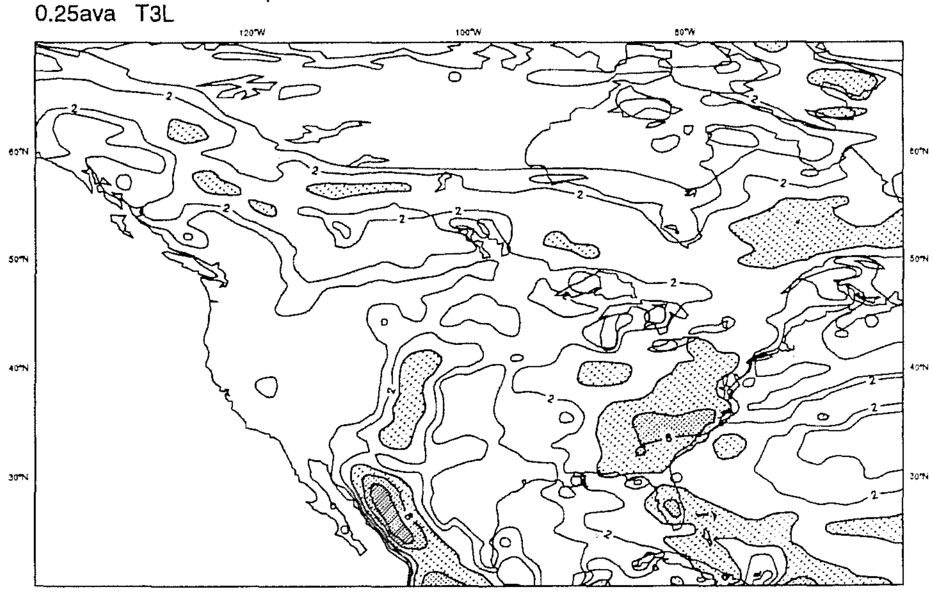

Fig 6 As Fig 5 for forecast initialised with dry soil moisture, corresponding to stressed evaporation.

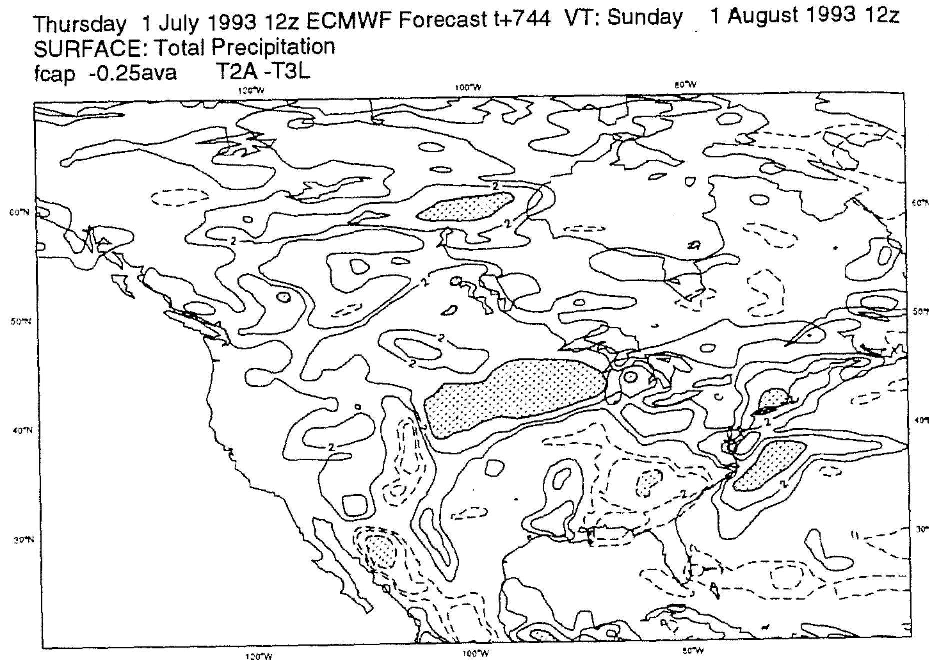

Fig 7 Difference (Fig 5-Fig 6) showing increase in montlhy mean precipitation resulting from increase in initial soil moisture.

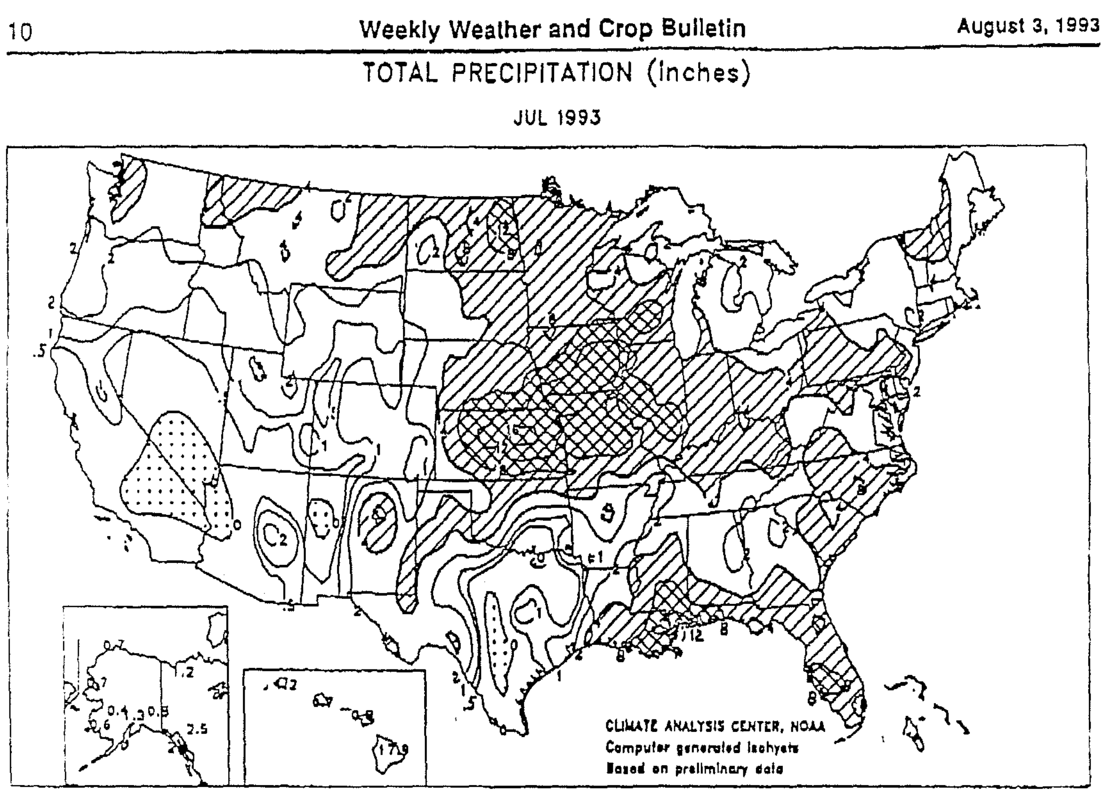

Fig 8 NOAA Climate Analysis Centre map of observed July precipitation in inches.

accepted).
Betts, A.K., J.H. Ball, and A.C.M. Beljaars, 1993: Comparison between the land surface response of the European Centre model and the FIFE-1987 data. Q.J.R.M.S., 119, 975-1001.
Carson, D.J., The development of a dry inversion-capped convectively unstable boundary layer, Q.J.R. Meteorol. Soc., 99, 450-467, 1973.
Kim J. and S.B. Verma, Components of surface energy balance in a temperate grassland ecosystem. Bound.-Layer Meteor., 51, 401-417, 1990.
Miller, M.J., A.C.M. Beljaars and T.N. Palmer, 1992: The sensitivity of the ECMWF model to the parameterization of evaporation from the tropical oceans. J. Clim., 5, 418-434.
Sellers, P.J. and F.G. Hall, FIFE in 1992: Results, Scientific Gains, and Future Research Directions, J. Geophys. Res., pp 19091-19109, 1993.
Smith, E.A., W.L. Crosson, and B.D. Tanner, 1992: Estimation of surface heat and moisture fluxes over a prairie grassland. In situ energy budget measurements incorporating a cooled mirror dewpoint hygrometer. J. Geophys. Res., 97, 18557-18582.
Tennekes, H., A model for the dynamics of the inversion above a convective boundary layer, J. Atmos. Sci., 30, 558-567, 1973.